



ELSEVIER

Available online at www.sciencedirect.com



Progress in Natural Science: Materials International 20(2010) 97–103

Progress in
Natural Science:
Materials
International

www.elsevier.com/locate/pnsc

Exploitation of shape memory alloy actuator using resistance feedback control and its development

Hiroki CHO¹, Takaue YAMAMOTO², Yuji TAKEDA², Akihiko SUZUKI¹, Toshio SAKUMA¹

1. Faculty of Engineering, Oita University, 700 Dannoharu, Oita 870-1192, Japan;
2. TAKE R&D, 2-7-27, Umeda, Kasukabe, Japan

Received 23 August 2010; accepted 23 October 2010

Abstract: The relationship between phase transformation and electric resistivity of Ti-42.6Ni-7Cu SMA was investigated. In the isothermal tensile tests, stress—strain curve shows large hysteresis and nonlinearity, whereas the resistivity—strain curve can be fitted by linearity. The resistivity of SMAs can be determined from the volume fractions of the martensitic and austenitic phases. This characteristics leads to that the resistance of the SMAs is used as a parameter of strain of SMAs. A SMA actuator using resistance feedback control system was proposed, which can control and retain positioning at any positions without using sensor devices, and the deviation of position of this system was less than 3 μm.

Key words: Ti-Ni-Cu alloy; shape memory alloy; resistivity; shape memory characteristics; phase transformation

1 Introduction

Shape memory alloys (SMAs) are useful in various fields of engineering and medical because they exhibit excellent shape memory and mechanical properties[1]. SMAs are expected to be candidate materials of driving elements for small size actuators, because they have sense and respond functions to temperature; therefore, actuators using SMAs[2–3] do not need sensors, for example, temperature sensor. Ti-Ni-Cu SMAs are good candidate materials for actuators because they exhibit smaller transformation hysteresis than other SMAs[4–5]. Because SMAs have transformation hysteresis, it is difficult for SMA actuator to control and retain positioning at any positions without using sensor devices.

SMAs have electric resistance characteristics with phase transformations[6]. Therefore, authors have proposed the SMA actuator using resistance feedback control system[7–8]. For the establishment of this system, it is indispensable to investigate the relationship between phase transformation and electric resistivity of SMAs. Many other researchers have reported the effects of manufacturing processes on shape memory properties[9–15], and several have reported the resistance characteristics of SMAs[16–20]. However,

more systematic research on resistance characteristics is necessary for applying SMAs to actuators using resistance feedback control system. In this work, relationship between phase transformation and electric resistance (resistivity) of Ti-Ni-Cu shape memory alloy is investigated. A two-dimensional drive SMA actuator using resistance feedback control system is developed. This system can control and retain positioning at any positions without using sensor devices. And the positioning characteristic of this system is also investigated.

2 Experimental

The chemical composition of the alloy used in this work was Ti-42.6Ni-7Cu (molar fraction, %). The specimen was a wire with 0.3 mm in diameter and 150 mm in length, which was processed by making ingot in high-frequency induction vacuum furnace, and then subjected to hot-forging, hot-extruding, cold-drawing and intermediate annealing. The cold working (CW) ratio of the specimen was 30%. The specimen shows two-way shape memory effect because of the manufacturing process. Figure 1 shows the strain—temperature curves for the Ti-Ni-Cu alloy wire. The solid and dashed lines denote heating and cooling processes, respectively. During cooling, the strain increases with decreasing

Corresponding author: Hiroki CHO; E-mail: hirocho@oita-u.ac.jp

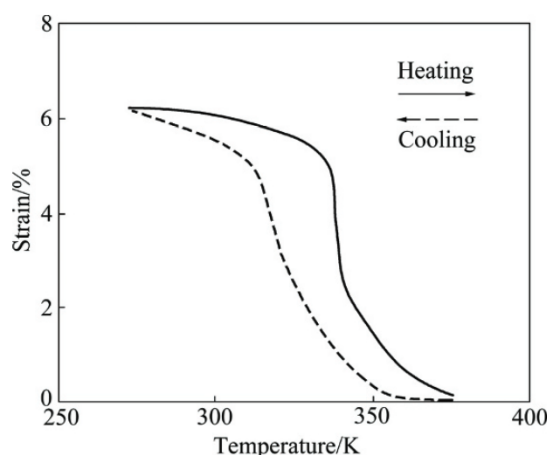


Fig.1 Strain—temperature curve of Ti-Ni-Cu wire under unloaded condition

temperature because of two-way shape memory effect; it decreases with increasing temperature during heating because of reverse transformation. Thus, this sample transforms from martensitic phase to austenitic phase and shows about 6% transformation strain under unloaded conditions.

Shape memory and electrical resistance properties were investigated by thermal cycling tests under constant stress and isothermal tensile tests. In thermal cycling tests under the constant stress, the temperature was increased from 300 to 373 K at a rate of 1 K/min in furnace, and the sample was cooled off at 300 K by furnace cooling. The applied stress was varied from 6 to 70 MPa, which was in appropriate stress range for SMA actuators. In isothermal tensile tests, the applied strain was varied from 3% to 8%, and the atmosphere temperature was 373 K. Transformation start temperature M_s , transformation finish temperature M_f , reverse transformation start temperature A_s and reverse transformation finish temperature A_f were measured by differential scanning calorimetry (DSC).

3 Results and discussion

3.1 Thermal cycling test

Figures 2 and 3 show the recovery strain—temperature and resistivity—temperature curves of the Ti-Ni-Cu wire under 70 MPa during thermal cycling test, respectively. The recovery strain—temperature curve shows transformation hysteresis, and the resistivity—temperature curve shows transformation hysteresis. The variation of resistivity is not caused by deformation but by the phase transformation because resistivity is calculated from the resistance, length and cross-sectional area. Generally, the resistivity of metal increases with

increasing temperature whether the metal is transformed or not. Therefore, it is necessary to fix the measurement temperature to determine the resistivity of the martensitic and austenitic phases. Regardless of stress, all specimens were completely martensitic and austenitic phase at 310 and 370 K during heating, respectively. Therefore, the resistivity of the martensitic and austenitic phases is obtained from the resistivity at 310 and 370 K during heating, respectively.

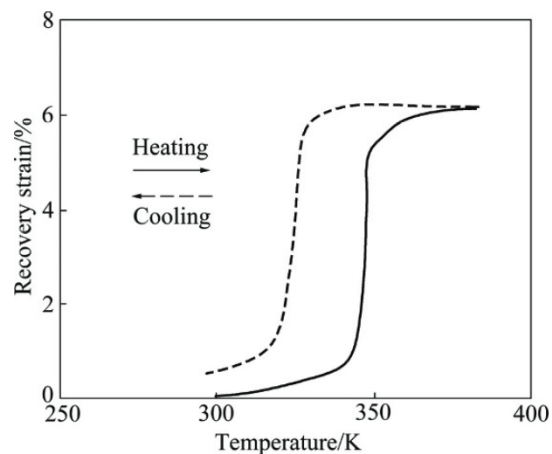


Fig.2 Recovery strain—temperature curve of Ti-Ni-Cu alloy under 70 MPa

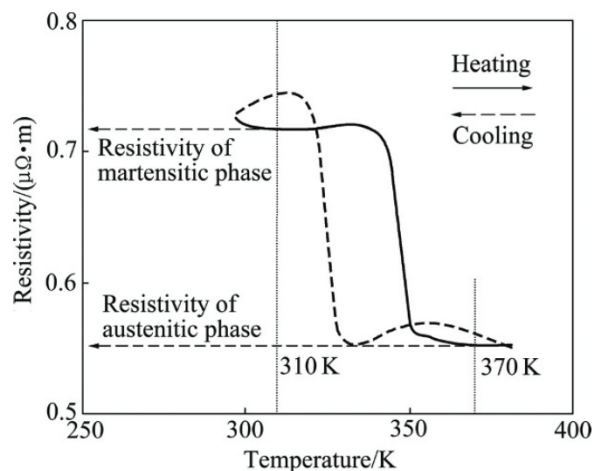


Fig.3 Resistivity—temperature curve of Ti-Ni-Cu alloy under 70 MPa

Figure 4 shows the effect of stress on the resistivity of martensitic and austenitic phases. The resistivity of martensitic phase is higher than that of austenitic phase. Additionally, the resistivity of each phase is approximately constant with varying stress. These results indicate that the resistivity of the martensitic phase is different from that of austenitic phases, and the resistance properties of the alloy do not vary with stress. A difference is considered to be a difference in crystal structure.

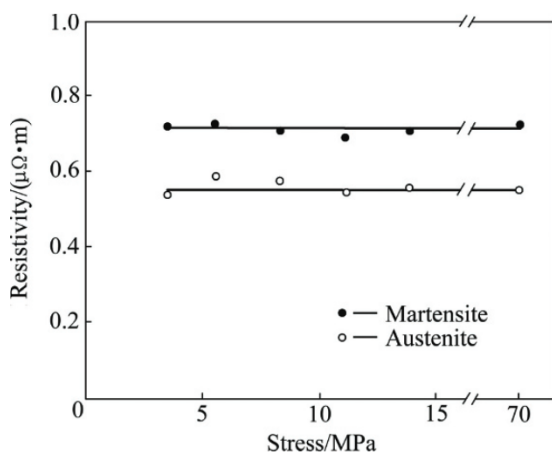


Fig.4 Effects of stress on resistivity for martensite and austenite phases of Ti-Ni-Cu alloy

Figure 5 shows the resistivity—recovery strain curve of the Ti-Ni-Cu wire under 70 MPa during thermal cycling test. Small hysteresis and linearity are observed. We suggest a hypothesis that the resistivity of SMA is determined from the volume fraction of martensitic and austenitic phases. Figure 6 shows a detailed description of the variation of resistivity in thermal cycling test. At room temperature, the specimen is martensitic phase. During heating, the recovery strain and volume fraction of austenitic phase increase with increasing the temperature. The increased volume fraction of austenitic phase causes a decrease of resistivity, because the resistivity of austenitic phase is lower than that of martensitic phase (see Fig.3). Cooling has a contrast effect on resistivity. Thus, resistivity varies with the volume fraction of each phase and the resistivity—recovery strain curve shows linearity.

If it is assumed that the resistivity of SMA is varied with the volume fraction of each phase, the resistivity—recovery strain curve can not show hysteresis. However, the resistivity—recovery strain curve shows a hysteresis

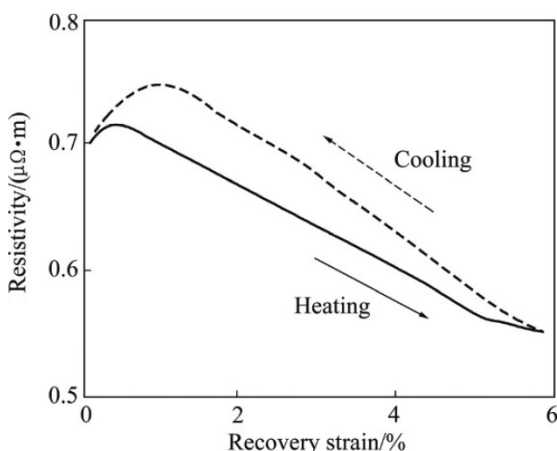


Fig.5 Resistivity—recovery strain curve of Ti-Ni-Cu alloy under 70 MPa

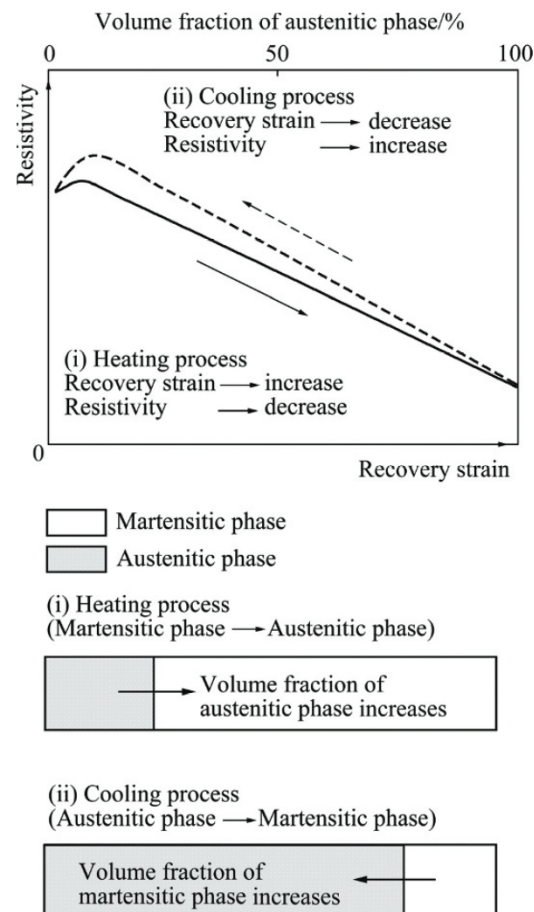


Fig.6 Detailed description of variation of resistivity of Ti-Ni-Cu alloy by phase transformation

although being small, as shown in Fig.5. As mentioned above, the resistivity of metal varies with varying temperature. Whereas the heating is carried out with 1 K/min, the cooling is carried out by furnace cooling. Therefore, it is thought that the hysteresis of resistivity—recovery strain curve is caused by the variation of resistivity which is due to the variation of temperature, because the atmosphere temperature and the cooling rate are different from the heating rate during the thermal cycling test.

3.2 Isothermal tensile tests

To confirm the hypothesis that the resistivity of SMA is determined from the volume fraction of each phase, isothermal tensile tests were carried out. Figure 7 shows the stress—strain curve and resistivity—strain curve during tensile test at 373 K. The applied strain is 3%. The specimen shows super-elastic behaviour because the atmosphere temperature is above A_f . The resistivity increases with increasing strain, and the resistivity—strain curve shows complete linearity. Moreover, the resistivity varies with strain during deformation of phase transformation, whereas the resistivity hardly varies during elastic deformation.

These facts suggest that the resistivity of SMA is varied with phase transformation and is determined from the volume fractions of austenitic and martensitic phases, because most of the variation of resistivity does not occur during elastic deformation but occurs during phase transformation.

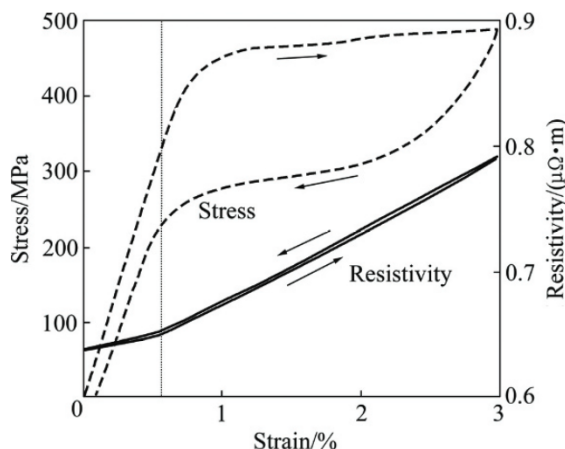


Fig.7 Stress—strain and resistivity—strain curves of Ti-Ni-Cu alloy wire during isothermal tensile test at 373 K

Figure 8 shows the stress—strain curve and the resistivity—strain curve during breaking test at 373 K. The breaking strain is about 11%, and the start and finish points of the transformation, inflection points of stress—strain curve, are about 1.2% and 8.2% strain, respectively. This indicates that the phase transformation occurs during 1.2%–8.2% strain. However, the inflection points of resistivity—strain curve are about 0.8% and 9.5% strain, indicating that the transformation start and finish points obtained by resistivity—strain curve are different from those points obtained by stress—strain curve. Moreover, this result suggests that the actual transformation start and finish points are ahead and behind the transformation start and finish points obtained from stress—strain curve, respectively.

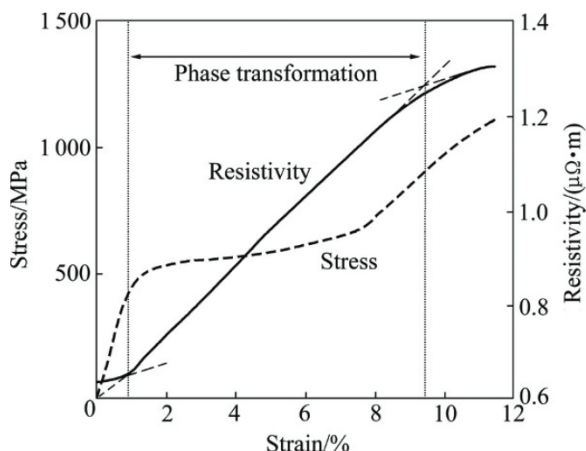


Fig.8 Stress—strain and resistivity—strain curves of Ti-Ni-Cu alloy wire during breaking test at 373 K

This finding agrees well with the simulation model of transformation of SMA[21]. Figure 9 shows the simulation of superelastic behavior of SMA. This simulation is calculated by the constitutive model describing the accommodation mechanism in the phase transformation process of polycrystalline SMA. The solid and dashed lines denote the deformation of phase transformation and elastic deformation, respectively. This simulation also suggests that the transformation start and finish points are ahead and behind the transformation start and finish points obtained from stress—strain curve, respectively. Thus, it is thought that the actual transformation start and finish points are different from transformation start and finish points obtained from stress—strain curve, respectively.

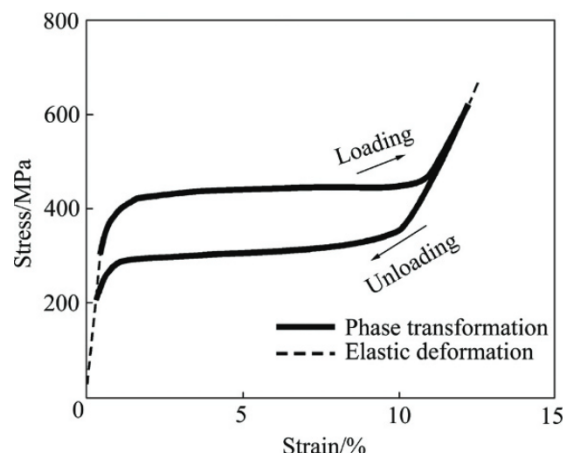


Fig.9 Simulation of superelastic behavior of SMA

3.3 SMA actuator using resistance feedback control

The resistivity of SMA is determined from the volume fractions of the martensitic and austenitic phases. Moreover, a linear relation is established between the resistance and strain of SMA. The resistivity—strain curve does not show hysteresis. This characteristics leads to that the resistance of the SMAs can be used as a parameter of strain of SMAs. Therefore, we proposed a SMA actuator using resistance feedback control system. Figure 10 shows a schematic drawing of the uniaxial driving SMA actuator using resistance feedback control system. This system is composed of SMA wire, a slider, a strain gauge and a position control unit. The SMA wire is Ti-Ni-Cu alloy and the dimension of wire is 0.15 mm in diameter and 200 mm in length. SMA wire in the state of martensitic phase is elongated by spring of strain gauge. The slider moves to the right side and left side by electric resistance heating and natural cooling, respectively. The controller always monitors the resistance of SMA wire, and the positioning control is carried out by the controlling of resistance of SMA wire. The strain gauge is used for only the measurements of the positioning characteristics. Thus, this resistance

feedback system can control and retain positioning at any positions without using sensor devices. The relationship between the resistance and strain of SMA (displacement), and the position stability of this system are investigated.

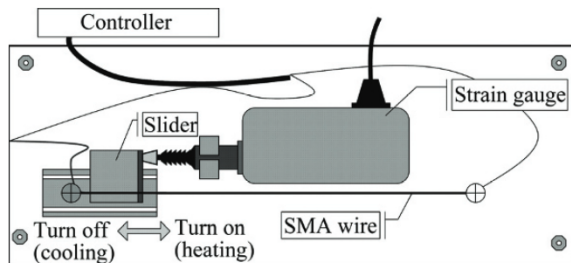


Fig.10 Schematic drawing of uniaxial driving SMA actuator using resistance feedback control system

Figure 11 shows the relationship between resistance and displacement of this system. It is a complete linearity regardless of heating and cooling. This simulation is calculated by the constitutive model mentioned above and the hypothesis that the resistivity of SMA is varied with the volume fractions of austenitic and martensitic phases. The simulation agrees well with the experimental result.

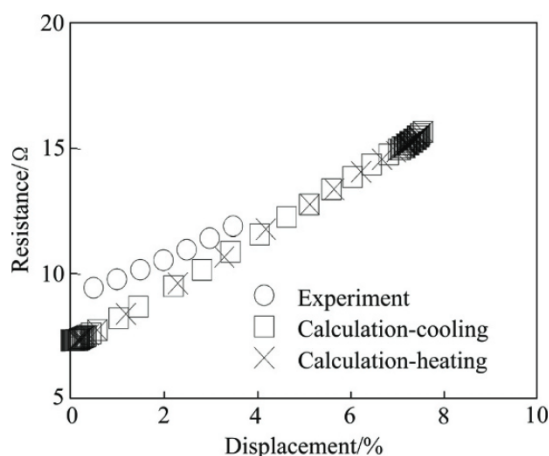


Fig.11 Variation of position stability with displacement

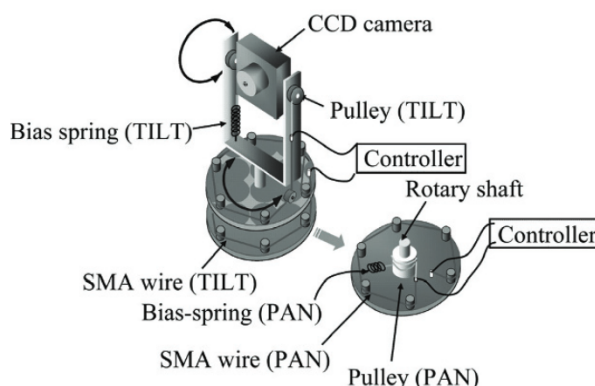


Fig.13 PAN/TILT camera-work SMA actuator using resistance feedback control system

Fig.12 shows the effect of the displacement (control distance) on the position stability of SMA actuator using resistance feedback control system. Deviation of position is calculated during positioning. The deviation of position slightly increases with the increasing of displacement. Thus, the position stability slightly decreases with the increasing of displacement. However, the deviation of position is always less than 3 μm . These indicate that the position control system used in this work has a constant stability despite of control distance, and the system has a good stability.

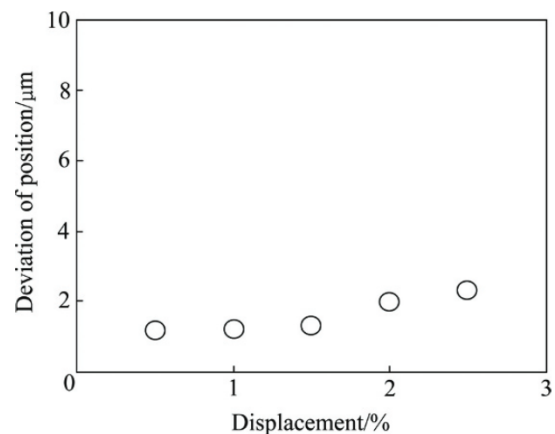
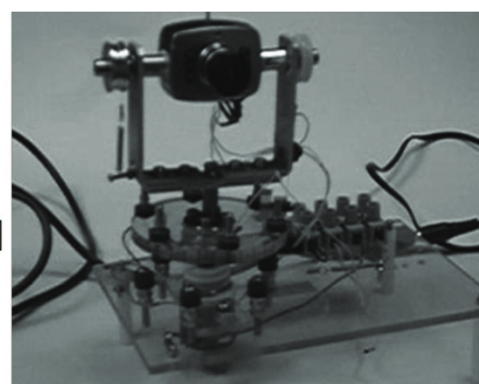


Fig.12 Variation of position stability with control distance

3.4 Trial products of SMA actuator using resistance feedback control system

Figure 13 shows the PAN/TILT camera work system. This system is composed of CCD camera, SMA wire, bias spring, pulley, rotary shaft and controller. This system uses neither the motor nor the gear. Therefore, this system is noiseless mechanically and electrically. By resistance feedback control, this camera can control and retain positioning at any position. Thus, PAN/TILT camera work to any position is possible in this system.

Figure 14 shows the *X-Y* table system. SMA wires and bias springs are installed in the tables of *X*-axis and *Y*-axis each. By resistance feedback control system, this



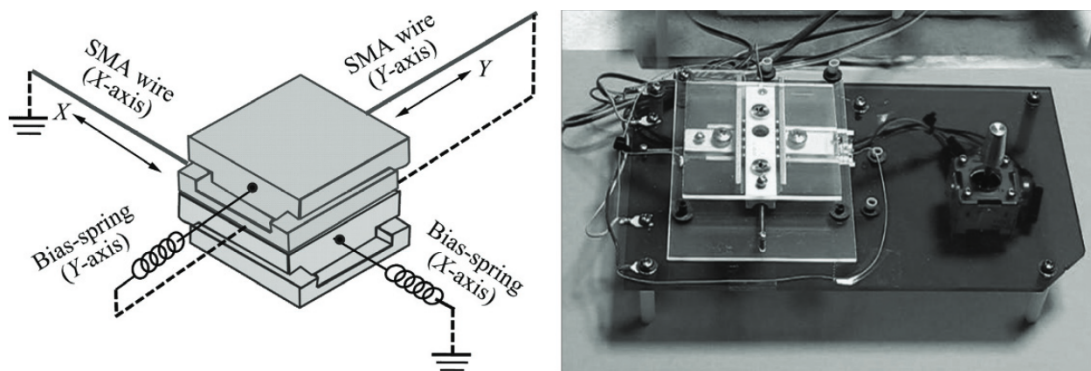


Fig.14 X-Y table SMA actuator using resistance feedback control system

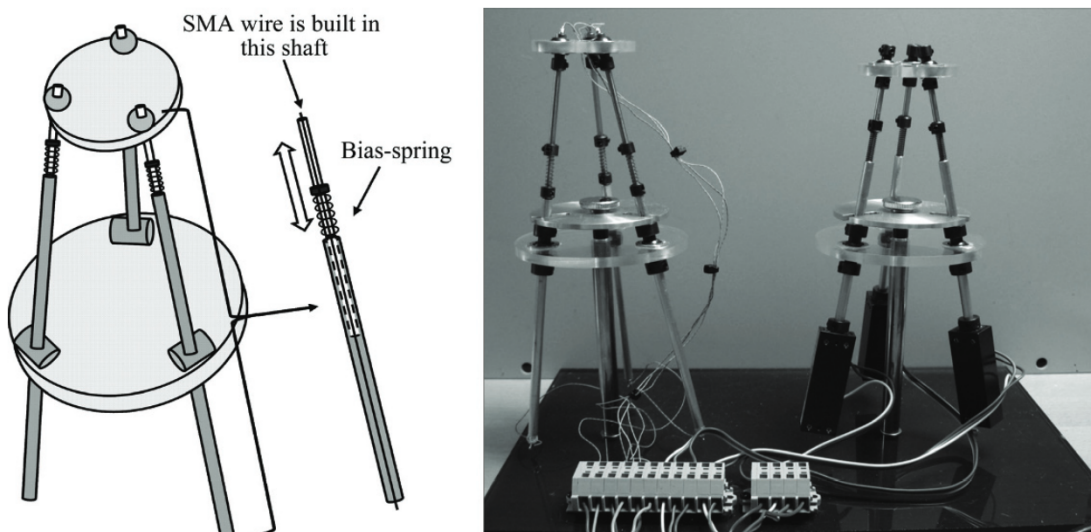


Fig.15 3-parallel-link SMA actuator using resistance feedback control system

X-Y table can do the biaxial movement: this system can control and retain positioning of 2 axes. Also, this system is noiseless mechanically and electrically, because this system uses neither the motor nor the gear.

Figure 15 shows the 3-parallel-link SMA actuator system. The SMA wire is built in the each shaft of the left side device. The potentiometer is built in the each shaft of the right side device. These shafts can expand and contract. When the right side device is moved by hand operation, its displacement of each shaft is measured by potentiometer. And then, the controller makes the shaft of left side device moving same amount of displacement measured by potentiometer. In other words, the left side device follows the right side one. The displacement of the left side device is also controlled by resistance feedback control. This system is expected for the remote control for example telemedicine.

4 Conclusions

1) In the heating-cooling tests under constant stress, the strain—temperature and resistivity—temperature curves of Ti-Ni-Cu alloy show large hysteresis and

nonlinearity. The resistivity—strain curves show small hysteresis and linearity. In the isothermal tensile tests, stress — strain curve shows large hysteresis and nonlinearity. In contrast, the resistivity—strain curve does not show hysteresis and shows linearity. The resistivity of martensitic phase in Ti-Ni-Cu alloy is larger than that of austenitic phase. The resistivity of martensitic and austenitic phases is constant irrespective of stress. It is supposed that the resistivity of SMAs can be determined from the volume fractions of the martensitic and austenitic phases. These lead to that the resistance of the SMAs can be used as a parameter of strain of SMAs.

2) The SMA actuator using resistance feedback control system is developed. The relationship between resistance and displacement of this system shows complete linearity regardless of heating and cooling. This system can control and retain positioning at any positions without using sensor devices, and the deviation of position of this system is less than 3 μm .

3) Transformation start and finish points obtained by resistivity—strain curve is different from those obtained by stress—strain curve. It is possible that the

transformation start and finish points are ahead and behind the transformation start and finish points obtained from stress—strain curve, respectively. This conclusion accords with the simulation by the constitutive model described the accommodation mechanism in the phase transformation process of polycrystalline SMAs.

References

- [1] MIYAZAKI S, ISHIDA A. Martensitic transformation and shape memory behavior in sputter-deposited TiNi-base thin films[J]. Mater Sci Eng A, 1999, 273–275: 106–133.
- [2] KOHL M, SKROBANEK K D, MIYAZAKI S. Development of stress-optimised shape memory microvalves[J]. Sensors and Actuators A: Physical, 1999, 72: 243–250.
- [3] MIYAZAKI S, HIRANO M, NO V H. Dynamic characteristics of diaphragm microactuators utilizing sputter-deposited TiNi shape-memory alloy thin film[J]. Mater Sci Forum, 2002, 349–395: 467–474.
- [4] MIYAZAKI S, MIZUKOSHI K, UEKI T, SAKUMA T, LIU Y. Fatigue life of Ti-50 at.% Ni and Ti-40Ni-10Cu (at.%) shape memory alloy wires[J]. Mater Sci Eng A, 1999, 273–275: 658–663.
- [5] SAKUMA T, IWATA U, TAKAKU H, KRIYA N, OCHI Y, MATSUMURA T. Fatigue life of Ti-Ni-Cu shape memory alloy under thermo-mechanical cyclic conditions[J]. Trans Japan Soc Mech Eng A, 2000, A66–664: 748–754.
- [6] CHNADRA K, PURDY G R. Observations of thin crystals of TiNi in premartensitic states[J]. J Appl Phys, 1968, 39: 2176–2181.
- [7] TAKEDA Y, YAMAMOTO T, SAKUMA T. Effect of bias load on positioning characteristics of shape memory alloy actuator based on resistance feedback control[J]. Trans Materials Research Society of Japan, 2007, 32: 635–638.
- [8] TAKEDA Y, KUDO Y, YAMAMOTO T, SAKUMA T. Position control characteristics of antagonism type SMA actuator based on resistance feedback control[J]. Trans Materials Research Society of Japan, 2008, 33: 877–880.
- [9] SABURI T. Modern development of titanium-nickel alloys with shape memory[J]. Metals and Technology, 1989, 59: 11–18.
- [10] TODOROKI T, TAMAURA H. Deformation behavior of a thermally cycled Ti-Ni alloy coil under an applied stress[J]. Jpn Inst Met, 1985, 50: 538–545.
- [11] SAKUMA T, MIHARA Y, TOYAMA H, CCHI Y, YAMAUCHI K. Effect of cold working on transformation and deformation behavior after pre-deforming in Ti-50 at%Ni shape memory alloy[J]. Materials Transaction, 2006, 47: 787–791.
- [12] MIYAZAKI S, et al. Engineering aspects of shape memory alloys[M]. DUERING T W, et al, ed. Butterworth-Heinemann Ltd., 1990.
- [13] NISHIDA M, ITAI I, KITAMURA K, CHIBA A, YAMAUCHI K. Effect of grain size of parent phase on twinning modes of B19' martensite in an equiatomic Ti-Ni shape memory alloy[J]. J de Phys Colloq C8, 1995, 5: 635–640.
- [14] KIM J I, MIYAZAKI S. Effect of nano-scaled precipitates on shape memory behavior of Ti-50.9at.%Ni alloy[J]. Acta Mater, 2005, 53: 4545–4554.
- [15] KHALIL-ALLAFI J, DLOUHY A, EGGELEER G. Ni₄Ti₃-precipitation during aging of NiTi shape memory alloys and its influence on martensitic phase transformations[J]. Acta Mater, 2002, 50: 4255–4274.
- [16] COLUZZI B, BISCARINI A, DI MASSOA L, MAZZOLAI F M, STAFFOLANI B, GUERRAB M, SANTOROB M, CERESARA S, TUISSI A. Phase transition features of NiTi orthodontic wires subjected to constant bending strains[J]. Journal of Alloys and Compounds, 1996, 233: 197–205.
- [17] UCHIL J, MOHANCHANDRA K P, KUMARA K G, MAHESH K K. Study of critical dependence of stable phases in Nitinol on heat treatment using electrical resistivity probe[J]. Mater Sci Eng A, 1998, 251: 58–63.
- [18] CUELLAR E L, GUENIN G, MORIN M. Thermal analysis of the effect of aging on the transformation behaviour of Ti-50.9at.% Ni[J]. Mater Sci Eng A, 2003, 358: 350–355.
- [19] CUELLAR E L, GUENIN G, MORIN M. Behaviour of strain-resistivity coupled measurements of Ti-Ni-Cu wires during thermal cycling under constant stress[J]. Mater Sci Eng A, 2004, 378: 115–118.
- [20] WU S K, LIN H C, LIN T Y. Electrical resistivity of Ti-Ni binary and Ti-Ni-X (X = Fe, Cu) ternary shape memory alloys[J]. Mater Sci Eng A, 2006, 438–440: 536–539.
- [21] CHO H, SUZUKI A, SAKUMA T. Interaction surface of phase transformation stress by constitutive model for accommodation of transformation strain[J]. Trans Materials Research Society of Japan, 2010, 35: 359–363.